IEEE Access
Multidisciplinary ⋮ Rapid Review ⋮ Open Access Journal

Received July 21, 2018, accepted August 17, 2018, date of publication September 24, 2018, date of current version October 17, 2018.

Digital Object Identifier 10.1109/ACCESS.2018.2870903

Optimization of an Air Filled Compact Re-Entrant Coaxial Resonator for a C-Band Bandpass Filter

CHRISTOPHE HALLET[1], JEAN-FRANÇOIS FAVENNEC[1], (Member, IEEE), ÉRIC RIUS[1], (Senior Member, IEEE), JESSICA BÉNÉDICTO[1], LUDOVIC CARPENTIER[2], (Member, IEEE), AND DAMIEN PACAUD[3]

[1]Lab-STICC, 29238 Brest, France
[2]Centre spatial de Toulouse, 31401 Toulouse, France
[3]Thales Alenia Space, 31100 Toulouse, France

Corresponding author: Christophe Hallet (christophe.hallet@univ-brest.fr)

This work was supported by the Centre National d'Études Spatiales (CNES).

ABSTRACT This paper proposes an enhanced model for a re-entrant coaxial resonator and analyzes the capacitance behavior between its different sections and the Q-factor, for which mathematical expressions are derived. This model makes it possible to carry out a geometric optimization to minimize the volume of a compact coaxial resonator. Theoretical conclusions are compared with electromagnetic simulations and an optimized symmetrical six-pole re-entrant coaxial resonator bandpass filter prototype is designed and fabricated to illustrate the optimization.

INDEX TERMS re-entrant coaxial resonator, SIR , C-band filter, frequency model, Q-factor model, optimization.

I. INTRODUCTION

Most fields of activity such as telecommunications, defense, and spatial technologies require small, low-cost microwave filters with high Q-factors and wide spurious-free performances. Furthermore, as reported in the literature, coaxial cavities with high Q-factors, capacitive loading at the input of the resonators to reduce their volume, and Stepped Impedance Resonators (SIR) [1] have wide spurious-free performances.

Compact coaxial resonators are based on coaxial cavities using the concept of re-entrant coaxial lines, introduced by Cohn [2], to establish couplers. Other re-entrant line configurations have been developed to design filters to create transmission zeros above the passband [3]. Thanks to its three re-entrant coaxial lines of the compact resonator described in [4], two SIR effects are established, inducing a reduction of the resonator's volume offering additional degrees of freedom for form factors compared with a uniform quarter-wave coaxial resonator.

The configuration of the compact re-entrant coaxial resonator described in [4] can be used to increase the first harmonic frequency, but is inefficient for obtaining a high quality factor. A better resonator configuration for a high quality factor and a wide spurious-free performance for BTS applications are presented in [5]. To demonstrate the potential of this compact resonator, the present paper develops numerical and analytical models of the resonant frequency, open end capacitance, and quality factor. From these models, the resonator's volume can be minimized while keeping the same advantages as in [5]. From this optimization, a symmetrical six-pole filter was fabricated in the C-band.

The development of a frequency model and Q-factor model of the compact resonator are presented in Section II. Using these models, Section III then focuses on the optimization of this resonator so as to reduce its volume. The last Section IV then presents the design of a C-band compact coaxial filter, simulations and experimental data.

II. MODEL OF THE RE-ENTRANT COAXIAL RESONATOR

A. DESCRIPTION OF THE RE-ENTRANT COAXIAL RESONATOR

Fig. 1 illustrates a re-entrant coaxial resonator based on three re-entrant coaxial lines that create three coaxial transmission lines, C_1, C_2, and C_3, of lengths l_1, l_2, and l_3, and characteristic impedances Z_1, Z_2, and Z_3, respectively, defined by

$$Z_1 = \frac{\eta_0}{2\pi\sqrt{\varepsilon_r}} Ln\left(\frac{R_1}{r_1}\right) \tag{1a}$$

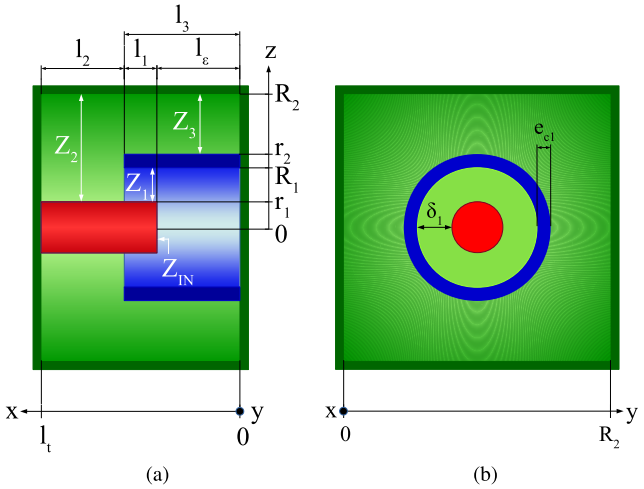

FIGURE 1. Structure of a re-entrant coaxial resonator. (a) Front view 1 - cross section. (b) Front view 2 - cross section.

$$Z_2 = \frac{\eta_0}{2\pi\sqrt{\varepsilon_r}} Ln\left(s\frac{R_2}{r_1}\right) \tag{1b}$$

$$Z_3 = \frac{\eta_0}{2\pi\sqrt{\varepsilon_r}} Ln\left(s\frac{R_2}{r_2}\right) \tag{1c}$$

where,
ε_r is the relative dielectric constant of the material,
η_0 is the vacuum impedance.
where the parameter s is defined by

$$s = \begin{cases} 1, & \text{for a circular section of radius } R_2 \\ 1.079, & \text{for a square section of half side } R_2 \end{cases}$$

The TEM signal propagation undergoes two SIR effects defined as $M_{12} = Z_2/Z_1$ and $M_{23} = Z_3/Z_2$ as well as a capacitive effect due to the capacitance C_{cap} defined by the matrix

$$\begin{bmatrix} A_{cap} & B_{cap} \\ C_{cap} & D_{cap} \end{bmatrix}_{cap} = \begin{bmatrix} 1 & 0 \\ jC_{IN}\omega & 1 \end{bmatrix} \tag{2}$$

with

$$\omega = \beta c_0/\sqrt{\varepsilon_r}$$
$$\beta = \sqrt{\varepsilon_r}.2\pi/\lambda_0$$

where, λ_0 is the wavelength in free space,
c_0 is the light celerity in vacuum.
The frequency model of the re-entrant coaxial resonator (Fig. 2) is based on the *ABCD*-matrix defined by

$$\begin{bmatrix} A & B \\ C & D \end{bmatrix}_{res} = \begin{bmatrix} A_{cap} & B_{cap} \\ C_{cap} & D_{cap} \end{bmatrix}_{cap} \times \begin{bmatrix} A_1 & B_1 \\ C_1 & D_1 \end{bmatrix}_1 \times \begin{bmatrix} A_2 & B_2 \\ C_2 & D_2 \end{bmatrix}_2 \times \begin{bmatrix} A_3 & B_3 \\ C_3 & D_3 \end{bmatrix}_3 \tag{3}$$

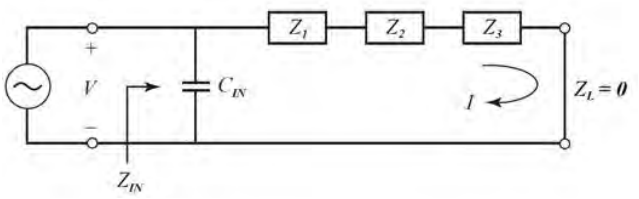

FIGURE 2. Electrical model of a re-entrant coaxial resonator.

where the ABCD-matrix of the lossless transmission line C_i is defined by

$$\forall i \in [\![1\,;3]\!]\,, \begin{bmatrix} A_i & B_i \\ C_i & D_i \end{bmatrix}_i = \begin{bmatrix} cos(\theta_i) & jZ_i sin(\theta_i) \\ \dfrac{jsin(\theta_i)}{Z_i} & cos(\theta_i) \end{bmatrix} \tag{4}$$

with l_i, the physical length of the i-th transmission line.
From Eq. 5 and Eq. 6, the resonant frequencies of the re-entrant coaxial resonator are calculated using the input impedance, Z_{IN}, with the shorted end of the resonator, Z_L, equal to zero.

$$Z_{IN} = \frac{A.Z_L + B}{C.Z_L + D} = \frac{B}{D} \tag{5}$$

where B and D are defined by

$$B = j\prod_{i=1}^{3} cos(\beta l_i)\{(Z_1 tan(\beta l_1) + Z_2 tan(\beta l_2)) + Z_3 tan(\beta l_3)[1 - (Z_1/Z_2)tan(\beta l_1)tan(\beta l_2)]\}$$

$$D = \prod_{i=1}^{3} cos(\beta l_i)\{[(1 - (Z_2/Z_1)tan(\beta l_1)tan(\beta l_2)) - Z_3 tan(\beta l_3)((tan(\beta l_1)/Z_1) + (tan(\beta l_2)/Z_2))] - (C_{IN}\omega)[Z_3 tan(\beta l_3)(1 - (Z_1/Z_2)tan(\beta l_1)tan(\beta l_2)) + (Z_1 tan(\beta l_1) + Z_2 tan(\beta l_2))]\}$$

Consequently, from the analytical expression of the input impedance Z_{IN}, the first zero of Eq. 6 can be found numerically as well as the first resonance, f_0, of the compact coaxial resonator.

$$1/Z_{IN}(r_1, R_1, r_2, R_2, l_1, l_2, l_3, C_{IN}) = 0 \tag{6}$$

Equation Eq. 6 shows that the input impedance Z_{IN} depends on geometrical parameters and the capacitance C_{IN}. Hence, a model of the capacitance C_{IN} is needed to obtain the first resonance f_0 of the resonator.
The parasitic inductance from the shorted end of the inner cylinders and the parasitic capacitance from the open end of the hollow cylinder are not studied in this paper.

B. MODEL OF THE CAPACITANCE C_{IN}

The behavior of the capacitance C_{IN} of the compact coaxial resonator can be described using three capacitance models of the inner cylinder of radius r_1:

- C^{plate}: capacitance between parallel surfaces;
- C^{fringe}: capacitance from the sidewall of the inner cylinder to another perpendicular surface [6];

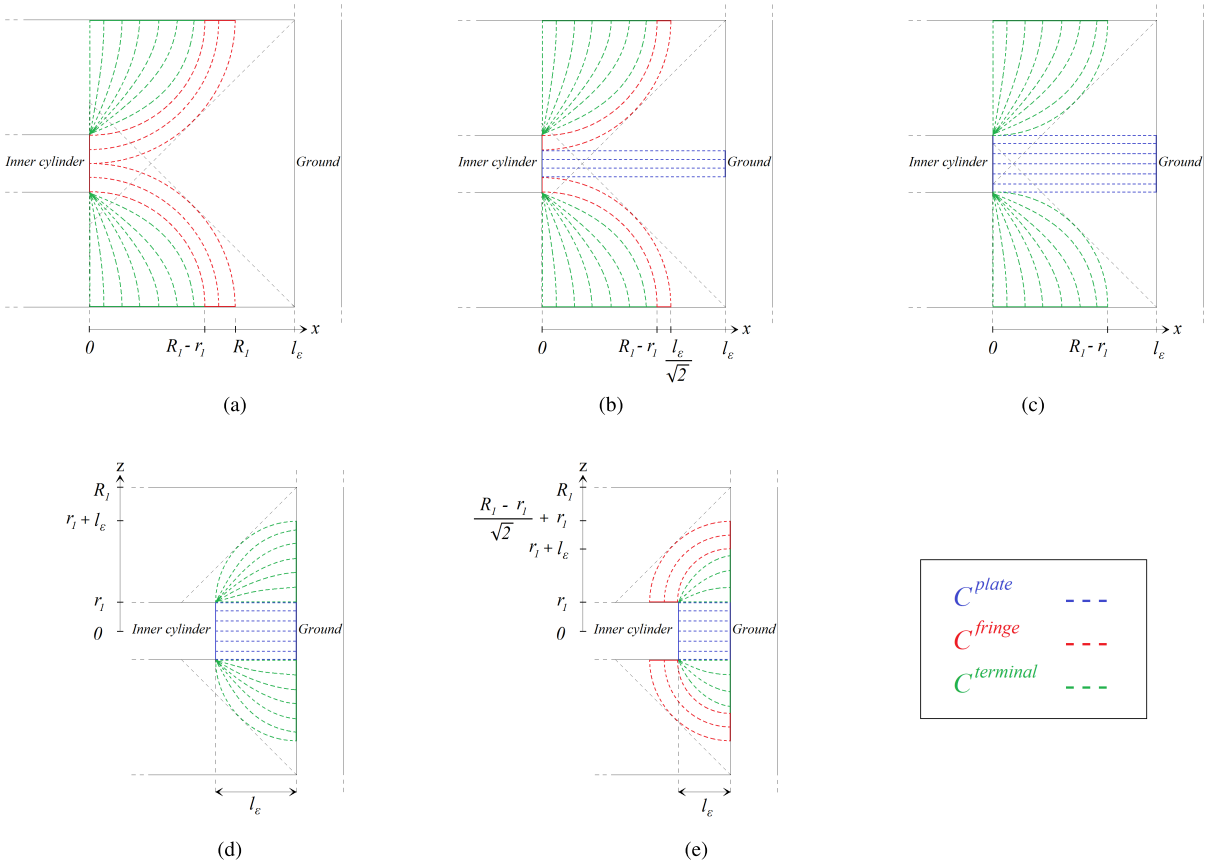

FIGURE 3. Electrical field of the capacitance C_{IN} for different lengths l_ε. (a) $R_1\sqrt{2} < l_\varepsilon \leq l_3$. (b) $(R_1 - r_1)\sqrt{2} < l_\varepsilon \leq R_1\sqrt{2}$. (c) $R_1 - r_1 < l_\varepsilon \leq (R_1 - r_1)\sqrt{2}$. (d) $\frac{R_1 - r_1}{\sqrt{2}} < l_\varepsilon \leq R_1 - r_1$. (e) $0 < l_\varepsilon \leq \frac{R_1 - r_1}{\sqrt{2}}$.

- $C^{terminal}$: capacitance from the corner of the inner cylinder to other surfaces [7].

Depending on the length l_ε separating the input of the open end cylinder from the ground, five different configurations of the capacitance C_{IN} can be identified: when the distance l_ε is low, the electrical field is concentrated between the open end and the ground, and when the distance l_ε is higher, the electrical field is more concentrated between the inner cylinder and the hollow cylinder (Fig. 3). Consequently, each configuration gives different values of the capacitances C^{plate}, C^{fringe} and $C^{terminal}$.

In order to simplify the notations of the capacitance C^{fringe}, the function f [6] is defined by Eq. 7.

$$\forall K \in]1; +\infty], \; f(K) = Ln\left(K^{2K^2}.\left(K^2 - 1\right)^{1-K^2}\right) \tag{7}$$

The capacitance C_{IN} is then determined by Eq. 8, as shown at the bottom of this page, where the dielectric constant ε is defined by

$$\varepsilon = \varepsilon_0 \varepsilon_r$$

where ε_0 is the dielectric constant in vacuum.

Hence, a solver is used to find the first resonant frequency of the re-entrant coaxial resonator from Eq. 6.

C. UNLOADED - Q_0

The unloaded Q_0 factor is determined to optimize the parameters of the re-entrant coaxial resonator as follows:

$$Q_0 = \frac{Q_c}{1 + Q_c \tan d} \tag{9}$$

$$C_{IN} = \begin{cases} 4\varepsilon r_1 + \varepsilon\dfrac{\pi r_1^2}{l_\varepsilon} + (2r_1\varepsilon).f(K), & 0 < l_\varepsilon \leq \dfrac{R_1 - r_1}{\sqrt{2}} \text{ and } K = \dfrac{\frac{R_1 - r_1}{\sqrt{2}} + r_1}{r_1 + l_\varepsilon} \\ 4\varepsilon r_1 + \varepsilon\dfrac{\pi r_1^2}{l_\varepsilon}, & \dfrac{R_1 - r_1}{\sqrt{2}} < l_\varepsilon \leq (R_1 - r_1)\sqrt{2} \\ 4\varepsilon r_1 + \varepsilon\dfrac{\pi}{l_\varepsilon}\left(R_1 - \dfrac{l_\varepsilon}{\sqrt{2}}\right)^2 + (2R_1\varepsilon).f(K), & (R_1 - r_1)\sqrt{2} < l_\varepsilon \leq R_1\sqrt{2} \text{ and } K = \dfrac{l_\varepsilon}{(R_1 - r_1)\sqrt{2}} \\ 4\varepsilon r_1 + (2R_1\varepsilon).f(K), & R_1\sqrt{2} < l_\varepsilon \leq l_3 \text{ and } K = \dfrac{R_1}{R_1 - r_1} \end{cases} \tag{8}$$

where tan d is the material dielectric loss tangent, and Q_c is the ohmic resonator quality factor, which can be calculated by solving the electromagnetic field of the TEM mode [8], [9]:

$$\begin{aligned} Q_c = \frac{2}{\delta} &\{A_1B_1Ln(R_1/r_1) + A_2B_2Ln(sR_2/r_1) \\ &+ A_3Ln(sR_2/r_2)\} / \{A_1B_1\,(1/R_1 + 1/r_1) \\ &+ A_2B_2\,(1/\,(sR_2) + 1/r_1) + A_3\,(1/\,(sR_2) + 1/r_2) \\ &+ 4\beta\,[Ln(sR_2/r_2) + B_2Ln(sR_2/r_1) \\ &+ \ B_3Ln(r_2/R_1)]\} \end{aligned} \tag{10}$$

where δ is the skin depth and

$$\begin{aligned} A_1 &= 2\beta l_1 - \sin(2\beta l_1) \quad B_1 = \frac{\cos^2(\beta l_3)}{\sin^2(\beta l_1)} \\ A_2 &= 2\beta l_2 + \sin(2\beta l_2) \quad B_2 = \frac{\cos^2(\beta l_3)}{\cos^2(\beta l_2)} \\ A_3 &= 2\beta l_3 + \sin(2\beta l_3) \quad B_3 = \cos^2(\beta l_3) \end{aligned}$$

III. C-BAND COMPACT RE-ENTRANT RESONATOR

A. OPTIMIZATION PROGRAM

Knowing the geometrical parameters of the compact coaxial resonator, the first resonant frequency, f_0, and the quality factor, Q_0, are calculated using Eq. 6 and Eq. 10. However, in order to design a resonator, the values of f_0 and Q_0 are given and the geometrical parameters need to be determined. Because of the complex formulation of the capacitance expression, a numerical program was developed to solve this problem.

From specified data, the program is described by an initialization, and while and for loops defined by six steps:

1) The specified data are given by the first resonant frequency f_0, the quality factor Q_0, the conductivity σ, and the thickness of the hollow cylinder $e_{c1} = r_2$-R_1.

2) The initialization is based on a set of given parameters: r_1, r_2 and l_t. The determination of the last parameters, R_2 and L, are realized in the case where the capacitance C_{IN} is neglected ($C_{IN} = 0$). Firstly, defining the conditions of the transmission line lengths by Eq. 11 and Eq. 12, the length L can be determined using Eq. 6 and Eq. 10.

$$l_1 + l_2 = l_3 = L \tag{11}$$

$$l_2 + l_3 = l_t \quad with\ l_1 \geq 0 \tag{12}$$

The radius R_2 of the resonator section and the quality factor Q of the numerical program are then initialized from 10.

3) In order to obtain a $Q = Q_0$ convergence, a while loop is realized on the parameter Q, and so :

$$\left.\begin{array}{l} if\ Q < Q_0 \\ if\ Q > Q_0 \end{array}\right\} then\ (Q_0/Q)R_2 \rightarrow R_2$$

From Eq. 6 and without neglecting the capacitance C_{IN}, the parameter L is updated and so, the resonator's volume is calculated for the set of given parameters r_1, r_2 and l_t.

4) At the end of each while loop, the resonator's volume is saved for each set of values (r_1, R_1, r_2, R_2, L, l_t).

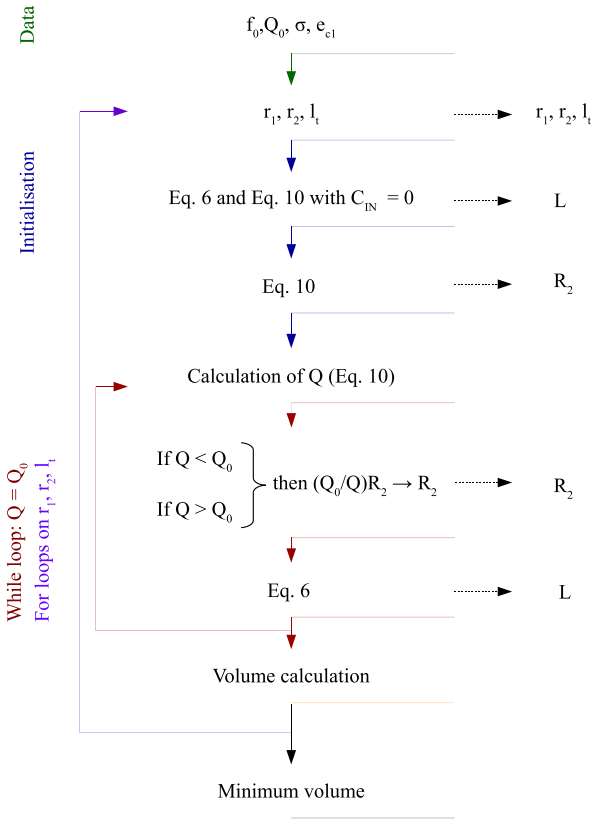

FIGURE 4. Schema of the numerical program.

5) A for loop is realized by changing the set of parameters r_1, r_2 and l_t. The parameters L and R_2 are then updated from steps 2) and 3), and a new volume is calculated.

6) Lastly, the minimum volume of the resonator is selected from the saved volumes.

The numerical program can optimize the six parameters (r_1, R_1, r_2, R_2, L, l_t) of the compact coaxial resonator for a given fundamental frequency f_0 and a given quality factor Q_0 in order to minimize the resonator's volume.

B. RESONATOR OPTIMIZATION

The C-band resonator design was realized at the fundamental frequency $f_0 = 7$ GHz and a conductivity of $\sigma = 45.10^6 S/m$. The resonator cylinder lengths were given by 11 and Eq. 12, the relative permittivity was equal to unity, the section of the resonator was square, and the thickness corresponded to $e_{c1} = 0.2$ mm.

The minimization volume of the C-band resonator was realized from the numerical program described previously for different values of the quality factor. The results of the optimization, based on the distance $\delta_1 = R_1$ - r_1, are illustrated in Fig. 5.

Fig. 5a shows how, first of all, when the frequency f_0 and quality factor Q_0 are given and when the distance δ_1 is arbitrarily imposed, the radius R_2 can be determined. Furthermore, increasing the radius R_2 involves increasing the

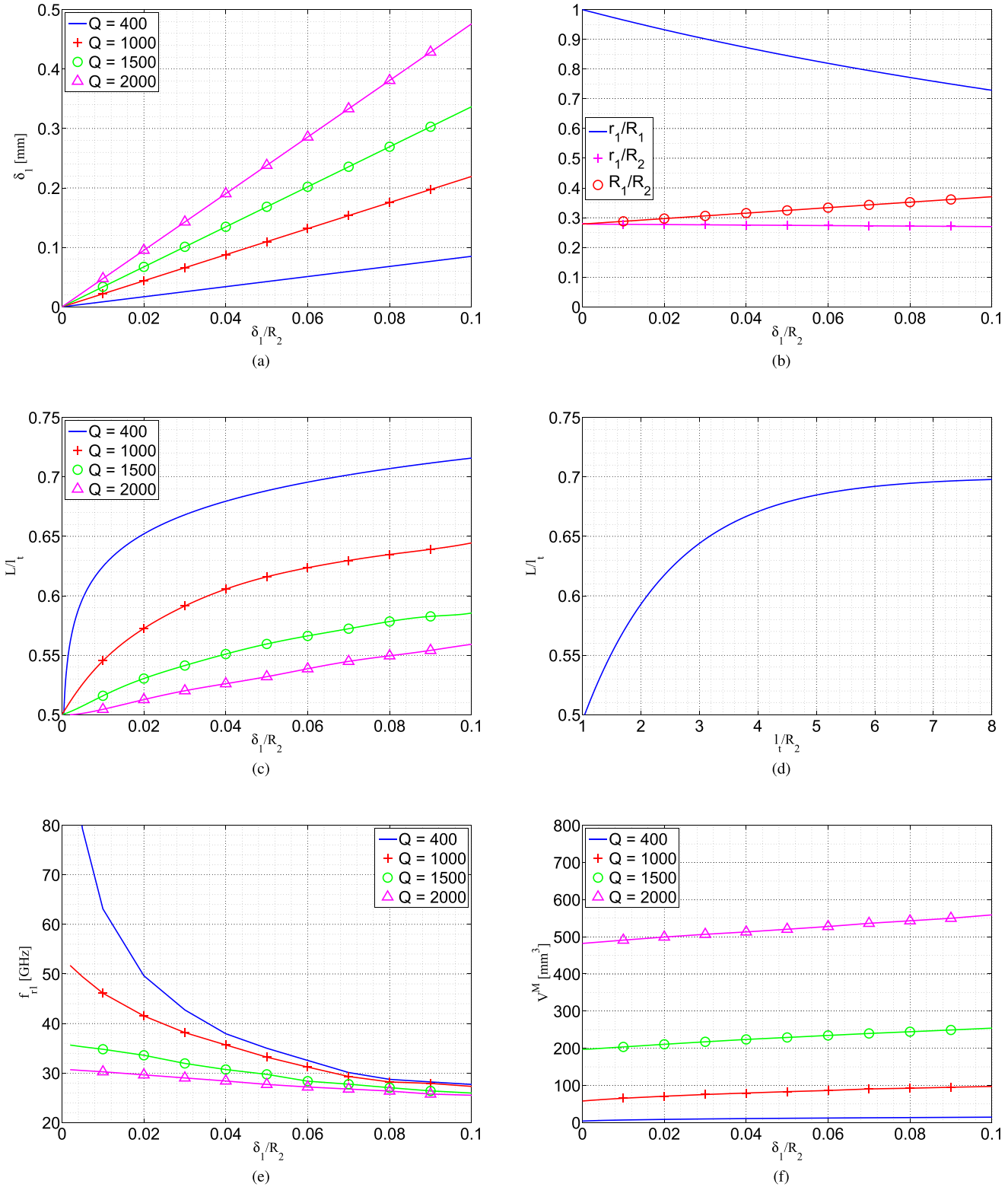

FIGURE 5. *Q*-factor optimization of a re-entrant coaxial resonator at $f_0 = 7$ GHz for $\sigma = 45.10^6 S/m$.

quality factor Q_0 for a distance δ_1 and a frequency f_0. This quality factor increase is directly linked to the increasing of the stocked electromagnetic field.

Then, when the radius R_2 is determined, the other radii r_1 and R_1 of the inner cylinders can be found for any quality factor value (Fig. 5b). These evolutions are

represented by

$$R_1 = 0.28R_2 + 0.92\delta_1 \quad (13a)$$

$$r_1 = 0.28R_2 - 0.085\delta_1 \quad (13b)$$

From these relations, when the distance δ_1 is equal to zero ($r_1 = R_1$), the compact coaxial resonator becomes a half-wavelength coaxial resonator and the optimal radius ratio r_1/R_2 becomes equal to 0.28, involving a characteristic impedance of 77 Ohms.

The total length l_t of the compact coaxial resonator and the length L of the inner cylinders can be determined using Fig. 5c and Fig. 5d. From Fig. 5c, when the ratio δ_1/R_2 is given, an increase of the quality factor involves a decrease of the ratio L/l_t, and the quality factor reaches a maximum when the ratio L/l_t is equal to 0.5. This minimum ratio corresponds to the limit of the compact coaxial resonator, i.e., the length l_1 is equal to zero and $l_2 = l_3$.

For a fundamental frequency and quality factor, a degree of freedom exists for the compact coaxial resonator design, which is the distance δ_1 separating the inner cylinder from the hollow cylinder. This distance δ_1 influences the first harmonic f_{r1}: the lower the distance, the higher the first harmonic (Fig. 5e). Furthermore, for a fundamental frequency and quality factor, the optimization means that for each value of δ_1, there is a single group of parameters (r_1, R_1, R_2, L, l_t), which minimizes the compact coaxial resonator's volume V^M (Fig. 5f). In this case, an overall volume exists for the resonator when the distance δ_1 approaches to zero.

Thanks to the frequency and the quality factor models, therefore, the minimization of the re-entrant coaxial resonator volume can be realized for any fundamental frequency f_0 and quality factor Q_0, and this minimization depends directly on the δ_1 value.

C. COMPARISON WITH A UNIFORM COAXIAL RESONATOR

In order to show the potential of the re-entrant coaxial resonator technology, the factor F, representing the degree of miniaturization of the compact coaxial resonator compared with a uniform quarter-wavelength coaxial resonator, is defined by

$$\forall \delta_1 > 0, F(\delta_1) = \frac{V^M(\delta_1) - V^{coax}}{V^{coax}} \quad (14)$$

where V^{coax} is the uniform quarter-wavelength coaxial resonator volume. The two resonator technologies can be compared with minimized volumes at the frequency $f_0 = 7$ GHz, i.e., the configuration of the coaxial resonator is given for a characteristic impedance equal to 77 Ohms, and the re-entrant coaxial resonator volume depends on the optimization of the development work in Section III.

The compact coaxial resonator volume is determined from Fig. 5f and compared with the uniform quarter-wavelength coaxial volume. This comparison is illustrated in Fig. 6, which represents the evolution of the re-entrant coaxial resonator volume compared with the uniform quarter wavelength coaxial resonator volume by the F-factor, as a function of the distance δ_1. This comparison shows an evolution of this F-factor for several quality factor values at the frequency $f_0 = 7$ GHz. Consequently, the F-factor decreases as the distance δ_1 decreases.

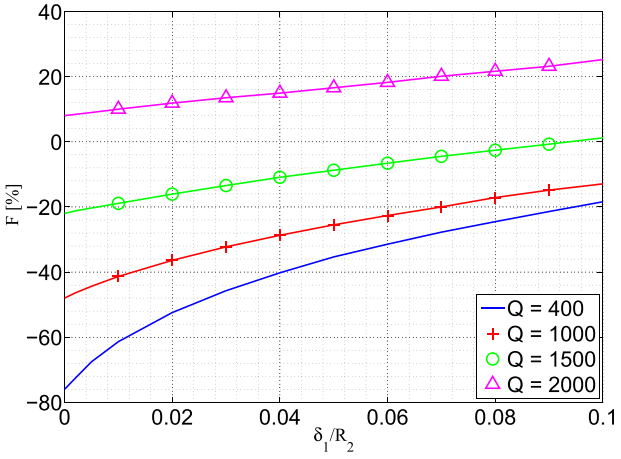

FIGURE 6. Evolution of the F factor at $f_0 = 7$ GHz for $\sigma = 45.10^6 S/m$.

The first harmonic frequency of the compact coaxial resonator illustrated in Fig. 5e is superior to the first harmonic frequency of the quarter-wavelength coaxial resonator, which is equal to $3f_0 = 21$ GHz.

Consequently, the decrease in the re-entrant coaxial resonator volume compared with the uniform quarter wavelength coaxial resonator volume is possible without degrading the quality factor for a given fundamental frequency. Furthermore, the lower the distance separating the inner cylinder from the hollow cylinder, the higher the decrease in the re-entrant coaxial resonator volume and the higher the first harmonic value.

IV. C-BAND COMPACT COAXIAL FILTER

A. C-BAND FILTER SPECIFICATIONS

In order to show the potential of re-entrant resonator technology, a symmetrical six-pole bandpass Tchebychev filter was designed and manufactured to operate in C-band. The filter specifications were a fundamental frequency $f_0 = 6.55$ GHz, a relative bandpass $BP_r = 9.9\%$, insertion losses IL ≤ 0.3 dB, a return loss superior to 23 dB and a first harmonic frequency $f_{r1} > 24$ GHz. Fig. 7 illustrates the filter specifications within the band near the fundamental frequency.

The direct couplings were realized by irises and the coupling matrix M of the filter was

$$M = \begin{bmatrix} 0 & K_{IN} & 0 & 0 & 0 & 0 & 0 & 0 \\ K_{IN} & 0 & K_{12} & 0 & 0 & 0 & 0 & 0 \\ 0 & K_{12} & 0 & K_{23} & 0 & 0 & 0 & 0 \\ 0 & 0 & K_{23} & 0 & K_{34} & 0 & 0 & 0 \\ 0 & 0 & 0 & K_{34} & 0 & K_{23} & 0 & 0 \\ 0 & 0 & 0 & 0 & K_{23} & 0 & K_{12} & 0 \\ 0 & 0 & 0 & 0 & 0 & K_{12} & 0 & K_{IN} \\ 0 & 0 & 0 & 0 & 0 & 0 & K_{IN} & 0 \end{bmatrix}$$

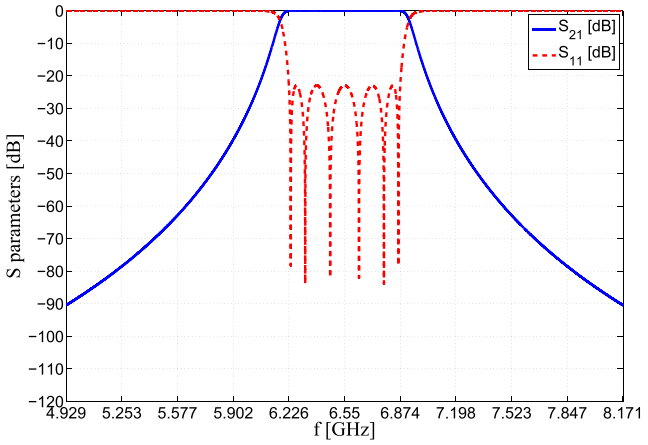

FIGURE 7. Ideal frequency responses of the C-band filter.

with $K_{IN} = 0.0473$, $K_{12} = 0.0891$, $K_{23} = 0.0626$ and $K_{34} = 0.594$.

To respect the insertion losses specification without modifying the bandpass or the return losses, the filter needed a quality factor of about 2000.

B. RESONATOR DESIGN

In order to minimize the compact coaxial filter volume, the resonator design was based on the optimization method developed in Section III. The resonator design was set at a fundamental frequency f_0 equals to 7 GHz instead of 6.55 GHz because the use of a coupling iris allows a decrease of the fundamental frequency of each resonator.

The quality factor Q_0 of the resonator was set at 2000 and the conductivity σ of the metallization was equal to 45.10^6 $S.m^{-1}$, realized by silver plating. The distance δ_1 separating the inner cylinder from the hollow cylinder was fixed at 0.24 mm in order to increase the first harmonic frequency up to 24 GHz. Furthermore, to minimize the resonator volume, the thickness e_{c1} of the hollow cylinder corresponded to 0.2 mm.

TABLE 1. Characteristic values of the re-entrant coaxial resonator vs HFSS® Results.

Initial data	Compact resonator	HFSS® Results
f_0 = 7.00 GHz	r_1 = 1.306 mm	f_0^{HFSS} = 6.97 GHz
Q_0 = 2000	R_1 = 1.544 mm	Q_0^{HFSS} = 2070
δ_1 = 0.238 mm	r_2 = 1.744 mm	f_{r1}^{HFSS} = 25.7 GHz
σ = 45.10^6 $S.m^{-1}$	R_2 = 4.761 mm	
e_{c1} = 0.2 mm	l_ε = 2.690 mm	
	L = 3.042 mm	

Based on the results of the optimization detailed in Section III, the geometrical parameters of the re-entrant coaxial resonator are given in Table 1, where the capacitance C_{IN} is obtained from Fig. 3. The electrical characteristics of the three transmission lines of the re-entrant coaxial resonator are given in Table 2.

TABLE 2. Electrical characteristics of the re-entrant coaxial resonator with C_{IN} = 0.1755 pF.

	Coaxial C_1	Coaxial C_2	Coaxial C_3
Z_i [Ohms]	10.04	82.13	64.78
l_i [mm]	0.352	2.69	3.042
β_i [rad/m]	146.71	146.71	146.71

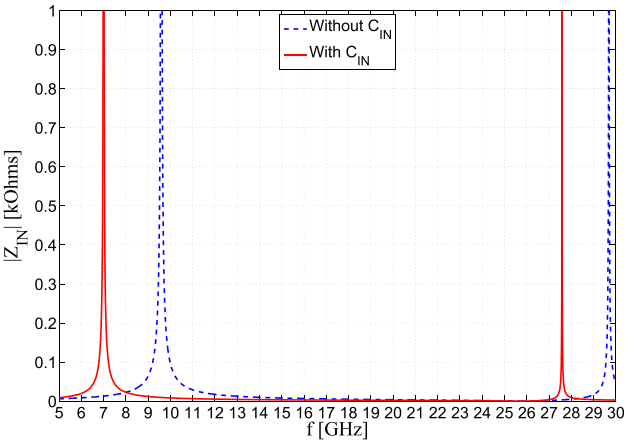

FIGURE 8. Impedance Z_{IN}.

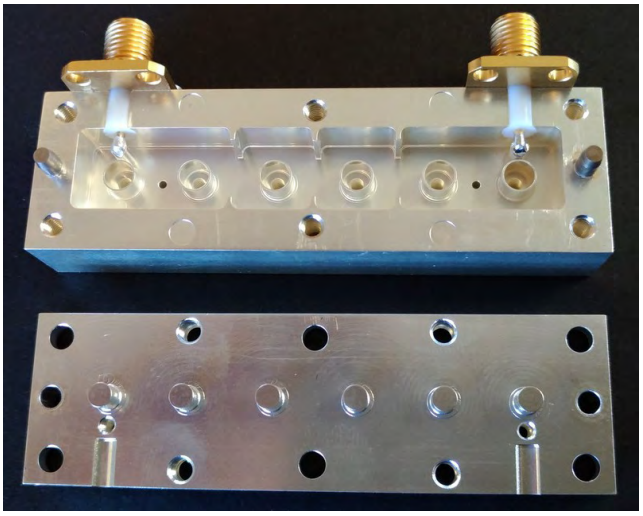

FIGURE 9. C-band filter.

The impedance Z_{IN} of the compact resonator is illustrated in Fig. 8 and shows that the frequency model of the re-entrant coaxial resonator depends on the model of the parasitic capacitance C_{IN}. Indeed, the frequency model of the resonator without the influence of the capacitance C_{IN} leads to a relative error of 37% for the fundamental frequency $f_0 = 7$ GHz.

The accuracy of the frequency and quality factor models is presented in Table 1. Indeed, an electromagnetic simulation carried out with the HFSS® software lead to similar results about the fundamental frequency and the quality factor as the initial data. Consequently, the frequency and quality factor models are accurate models of the re-entrant coaxial resonator in C-band. Hence, the parasitic inductance from the closed end of the inner cylinders and the parasitic capacitance

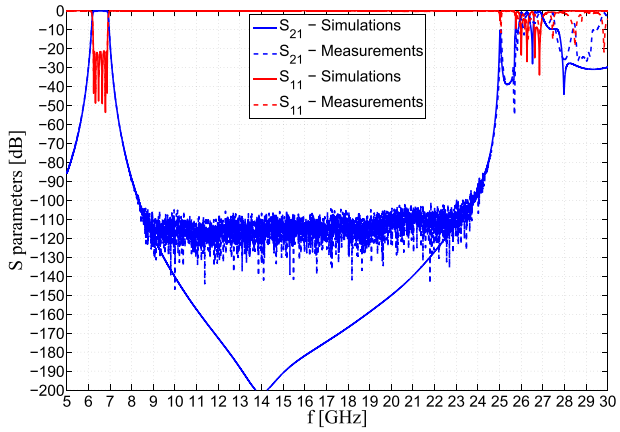

(a)

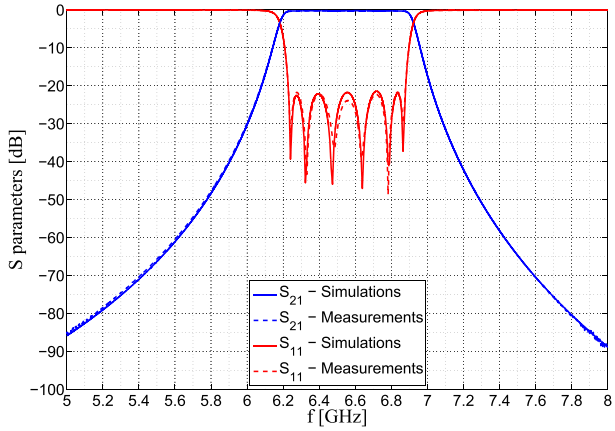

(b)

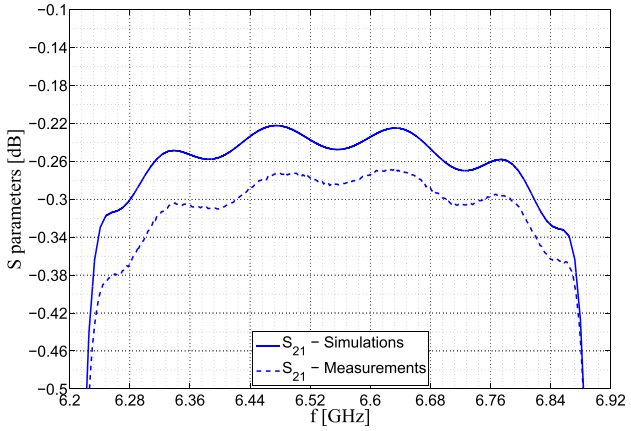

(c)

FIGURE 10. C-band filter measurements.

from the open end of the hollow cylinder can be ignored in this case.

The re-entrant coaxial resonator design produces HFSS® results corresponding to a fundamental frequency of $f_0 = 6.97$ GHz, a quality factor of $Q_0 = 2070$ and a first harmonic frequency of $f_{r1} = 25.7$ GHz. Consequently, this resonator configuration of physical length $\lambda/12.5$ was used to design the C-band filter.

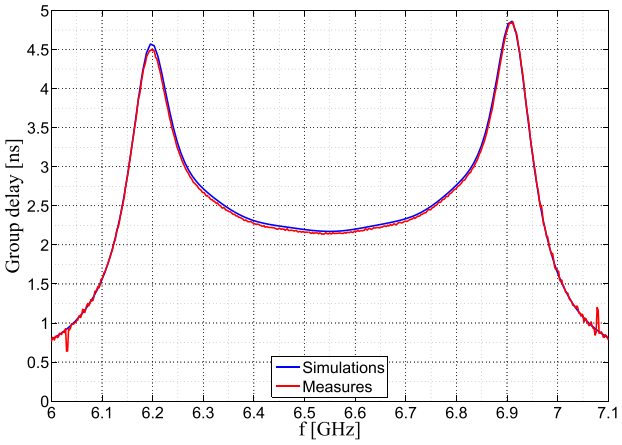

FIGURE 11. Group delay measurements.

C. FILTER DESIGN AND RESULTS

The C-band filter design was based on the re-entrant coaxial resonator configuration described in Table 1. Furthermore, the Tchebychev coupling matrix was respected adjusting the iris lengths separating the resonators, with the six resonators arranged along the same axis (Fig. 9). Eight tuning screws were placed within the manufactured filter to influence the resonant frequencies of the cavities and the coupling coefficient K_{01}.

The results of the electromagnetic measurements of the C-band filter are compared to the HFSS® simulations in Fig. 10, showing that the measurements and simulations of the transmission coefficient S_{21} are close. Indeed, the measured fundamental frequency, relative bandpass, and first harmonic frequency correspond to the simulated ones (Fig. 10a). Nevertheless, the insertion losses of the manufactured filter were higher than those predicted by the simulations. This difference was due to the underestimation of the losses of the filter's SMA connectors in the simulations (Fig. 10c).

The return losses results are different between the measurements and the simulations because the coupling coefficient K_{01} is superior to the coefficient of the theoretical coupling matrix (Fig. 10b). Despite the use of tuning screws to ensure this coupling coefficient, the soldering of the SMA connectors strongly influences the coupling coefficient.

Furthermore, the group delay measurement is also similar to the simulation. Consequently, the variations of the group delay in the band of the manufactured filter are equal to 0.6 ns.

Ultimately, the experimental responses of the manufactured filter were close to the simulated and theoretical responses.

V. CONCLUSION

A minimization of the re-entrant coaxial resonator volume was realized in C-band from analytical and numerical models of the resonant frequency and the quality factor. This resonator optimization was used to manufacture a six-pole filter in C-band. The C-band filter measurements were close to

the simulations, showing a higher wide spurious-free performance and offering a different form factor from a uniform quarter-wavelength coaxial resonator.

ACKNOWLEDGMENT

The authors would like to thank the company VUILLERMOZ PHILIPPE for manufacturing the filter.

REFERENCES

[1] M. Makimoto and S. Yamashita, "Bandpass filters using parallel coupled stripline stepped impedance resonators," *IEEE Trans. Microw. Theory Techn.*, vol. MTT-28, no. 12, pp. 1413–1417, Dec. 1980.

[2] S. B. Cohn, "The re-entrant cross section and wide-band 3-db hybrid couplers," *IEEE Trans. Microw. Theory Techn.*, vol. MTT-11, no. 4, pp. 254–258, Jul. 1963.

[3] E. Musonda and I. C. Hunter, "Microwave bandpass filters using re-entrant resonators," *IEEE Trans. Microw. Theory Techn.*, vol. 63, no. 3, pp. 954–964, Mar. 2015.

[4] H. Aouidad, E. Rius, J.-F. Favennec, A. Manchec, and Y. Clavet, "UHF second order bandpass filters based on miniature two-section SIR coaxial resonators," *Int. J. Microw. Wireless Technol.*, vol. 8, no. 8, pp. 1187–1196, 2016.

[5] E. Doumanis, S. Bulja, and D. Kozlov, "Compact coaxial filters for BTS applications," *IEEE Microw. Wireless Compon. Lett.*, vol. 27, no. 12, pp. 1077–1079, Dec. 2017.

[6] K. Suzuki, "Parasitic capacitance of submicrometer MOSFET's," *IEEE Trans. Electron Devices*, vol. 46, no. 9, pp. 1895–1900, Sep. 1999.

[7] W. Zhao, X. Li, S. Gu, S. H. Kang, M. M. Nowak, and Y. Cao, "Field-based capacitance modeling for sub-65-nm on-chip interconnect," *IEEE Trans. Electron Devices*, vol. 56, no. 9, pp. 1862–1872, Sep. 2009.

[8] S. Yamashita and M. Makimoto, "The Q-factor of coaxial resonators partially loaded with high dielectric constant microwave ceramics," *IEEE Trans. Microw. Theory Techn.*, vol. MTT-31, no. 6, pp. 485–488, Jun. 1983.

[9] M. Sagawa, M. Makimoto, and S. Yamashita, "A design method of bandpass filters using dielectric-filled coaxial resonators (short papers)," *IEEE Trans. Microw. Theory Techn.*, vol. MTT-33, no. 2, pp. 152–157, Feb. 1985.

CHRISTOPHE HALLET was born in Rennes, France, in 1991. He received the Diploma degree in telecommunications from the Engineer School, Institut National des Sciences Appliquées, Rennes, in 2015. He is currently pursuing the Ph.D. degree with the University of Brest. His research interests include the modeling and the conception of filters, and the study of the multipactor effect of filters for spatial applications.

JEAN-FRANÇOIS FAVENNEC received the Ph.D. degree in electronics from the University of Brest, Brest, France, in 1990. He received the Accreditation to Supervise Research (HDR) in 2016. He became an Assistant Professor with the École Nationale d'Ingénieurs de Brest, Plouzané, France, in 1991. He essentially teaches electromagnetic theory and microwaves. He currently conducts research with the Laboratoire en Sciences et Techniques de l'Information, de la Communication et de la Connaissance, Université de Bretagne Occidentale, Brest. His current research interests include the modeling and design of passive devices for microwave applications and are mainly focused on filters.

ÉRIC RIUS (SM'15) spent several months at Singapore as a Visiting Professor at Nanyang Technological University. He is currently a Professor with the University of Brest. He is also the Vice Head of the Lab-STICC UMR CNRS 6285. His research conducted at the Lab-STICC concerns the design of microwave passives devices for centimetric and millimetric wave applications. He is involved in many projects with the two French agencies ANR and CNES, and companies, such as Thales Alénia Space. He supervised over 20 Ph.D. students and several post-docs. He participated in over 90 Ph.D. jury defenses and 10 HDR jury defenses. In 2013, he was appointed by the European Microwave Association as a European Microwave Lecturer. In 2010, he was the TPC Chair of the 40th edition of the European Microwave Conference (over 5000 attendees). He has h-number 20, over 1800 citations, and most cited paper with 230 citations.

JESSICA BÉNÉDICTO received the Ph.D. degree in physics from the University of Blaise Pascal, Clermont-Ferrand, France, in 2013. During her Ph.D., she investigated the potential of metallo-dielectric multilayers, flat lens with sub-wavelength resolution, and non locality in metals. In 2013, she held a post-doctoral position at the Fresnel Institute, Marseille, France. The fields of applications were hybrid magnetic-electric dielectric scatterer near-field and far-field analyses. In 2015, she became an Assistant Professor with the Lab-STICC Laboratory, Brest, France. Her research interests are focused on the modeling and design of passive devices for microwave applications.

LUDOVIC CARPENTIER received the Ph.D. degree in electrical engineering from the University of Limoges, France, in 2012. He is currently a Research and Development Engineer with the French Space Agency (CNES), Toulouse, France, where he is involved in microwave passive components area.

DAMIEN PACAUD was born in France, in 1971. In 2001, he received the Ph.D. degree in Applied Mathematics and Scientific Computing from the University of Bordeaux 1, France. In 1996, he joined the CEG Center to develop powerful electromagnetic numerical techniques. In 2000, he joined IEEA, Paris, to develop RF software. Since 2001, he has been in charge of filters and multiplexers studies and developments for spatial applications at Thales Alenia Space, Toulouse, France. His main area of interest concerns optimization and computer-aided design processes for novel passive microwave products.